Applied Energy 297 (2021) 117091

Contents lists available at ScienceDirect

Applied Energy

journal homepage: www.elsevier.com/locate/apenergy

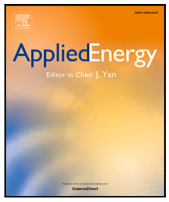

On the benefits of negative hydrodynamic interactions in small tidal energy arrays

Mathew B.R. Topper [a,*], Sterling S. Olson [b], Jesse D. Roberts [b]

[a] Data Only Greater, Maynooth, Ireland
[b] Sandia National Laboratories, Albuquerque, United States

ARTICLE INFO

Keywords:
Tidal energy converter
Arrays
Levelized cost of energy
Optimisation
Techno-economic modelling
DTOcean

ABSTRACT

As the technology of hydrokinetic tidal energy conversion looks to exploit smaller markets in the wider 'blue economy', innovation is still required to ensure cost competitiveness with other energy sources. A typical assumption of existing techno-economic models of tidal energy converter (TEC) arrays is that TECs positioned to minimise negative hydrodynamic interactions will maximise economic return. That the number of TECs within an array should be chosen to maximise the annual energy production, follows from this assumption. To examine the validity of these assertions for small, area-constrained arrays, a hypothetical model of the relationship of levelised cost of energy (LCOE) to the mean mechanical annual energy production (MMAEP) is developed. The model exhibits three classes of behaviour, determined by the rate of energy lost to interactions as TECs are added to an optimally positioned array; significantly, only one class has greatest MMAEP corresponding to lowest LCOE. To test this model, a contemporary optimisation algorithm is added to the advanced ocean energy techno-economic simulation tool 'DTOcean' and applied to arrays of TECs constrained by a 2 ha deployment area. It is shown that the hypothetical LCOE model accurately describes the DTOcean results up to and including 12 TECs deployed. At 13 TECs deployed, the level of TEC interaction increases dramatically, invalidating the hypothetical model. Notably, however, the LCOE is shown to reduce significantly by allowing negative interactions between TECs, reducing by 47.8% from the best non-interacting array. Thus, subject to an improved understanding of the relationship between the environment, TEC reliability and costs, the results indicate that allowing negative interactions between TECs may increase the economically extractable resource of small area-constrained tidal energy sites.

1. Introduction

Hydrokinetic tidal current energy conversion transforms kinetic energy from tidally driven flows into electrical energy (see [1]). If proven economically viable, this technology can become part of the global effort to reduce carbon emissions and mitigate the impact of climate change [2]. Yet, the cost of tidal current energy remains high in comparison to other renewable energy technologies; even with advantageous learning rates, [3] found that, in the UK, tidal current energy would remain approximately 2 to 5 times more expensive than offshore wind for utility scale generation by 2050. Very large scale tidal current energy conversion (hundreds of MWs) may also significantly modify the environment [4] and reduce the economic viability (via modified flows) of other, nearby, tidal energy sites [5].

In order to overcome these important barriers to entry, recent focus has been on market opportunities other than utility scale electricity generation. In [6] off-grid applications for small and remote ('blue economy') communities are identified as markets where tidal current energy conversion can have positive economic and social benefits over high-cost polluting energy sources such as diesel generation. Sites that provide smaller scale tidal current energy resources are also more abundant than those considered to be utility scale (for instance, the average viable power production for every tidal current site identified in Ireland, in [7], is less than 30 MW). The challenge for applying tidal current conversion (where arrays of converters are deployed) to these markets is that small arrays are less economically efficient than larger ones. A technology agnostic metric used to measure the economic efficiency of energy generating plant is the levelised cost of energy (LCOE). The LCOE estimates the revenue per unit of electricity required to cover the costs of operating a plant over its lifetime and, thus, lower values are better. For the Tacoma Narrows strait, in the north-west US,

* Corresponding author.
E-mail addresses: mathew.topper@dataonlygreater.com (M.B.R. Topper), ssolson@sandia.gov (S.S. Olson), jdrober@sandia.gov (J.D. Roberts).

https://doi.org/10.1016/j.apenergy.2021.117091
Received 19 January 2021; Received in revised form 3 May 2021; Accepted 18 May 2021
Available online 27 May 2021

List of Abbreviations, Units and Nomenclature

$\mathbf{C}$	Costs incurred per year of operation
$\mathbf{E}$	Energy exported per year of operation
$\mathbf{x}_i$	Position of TEC i
C_{cap}	Array capacity factor
C_P	Rotor power coefficient
C_T	Rotor thrust coefficient
E	Array MMAEP
P_i	Power output for rotor i
P_i^0	Power output without interactions for rotor i
P_{rated}	TEC rated power
T_a	Number of hours in a year
c^0	Costs incurred prior to commencement
c^i	Costs incurred per annum
c_0	Fixed capital costs
c_e	Fixed operational costs per annum
c_m	Operational costs per TEC per annum
c_x	Capital costs per TEC
d	Discount rate
f_0	Optimisation global objective function
f_i	Function representing MDO discipline i
f_p	Optimisation penalty value
$f_{\max}$	Maximum expected value of f_0
n_0	Maximum number of TECs that array can support without interaction
$n_{0.5}$	Number of TECs for when output is half of the undisturbed value
n_r	Number of TEC rotors
n_s	Total number of RVFs
n_t	Number of years in project
n_x	Number of TECs
(p_1, p_2)	Array centre point
r	Minimum spacing between TECs
(t_1, t_2)	Parametric representation of the TEC deployment area
(x, y)	Projected map coordinates
(z^-, z^+)	TEC deployment depth range
$\mathbb{P}$	Probability of occurrence of a RVF
$\mathbb{c}$	Optimisation constraints
$\mathbb{k}$	Optimisation loop index
$\mathbb{n}$	Number of dimensions in optimisation search space
$\mathbb{q}$	Array q-factor
$\mathbb{q}_i$	q-factor for rotor i
$\mathbb{s}$	UH-CMA-ES uncertainty metric
$\mathbb{t}$	Number of function evaluations of the stochastic cost function
$\mathbb{t}_{\max}$	Maximum $\mathbb{t}$
$\mathbb{x}$	Optimisation design variables
$\mathbb{x}_{\text{feasible}}$	Feasible solution to f_0
$\mathbb{y}$	Optimisation coupling and state variables
Ω	TEC deployment area
Ω^*	Minimum-area enclosing rectangle of constrained deployment area
Θ	TEC positioning grid rotation
α_σ	Multiplier of σ
α_t	Multiplier of $\mathbb{t}_{\text{eval}}$
δ_c	TEC positioning grid column spacing
δ_r	TEC positioning grid row spacing
σ	Population variance of UH-CMA-ES solution search space
q-factor	Factor of power reduction due to interactions
CAPEX	Capital expenditure
CFD	Computational fluid dynamics
LCOE	Levelised cost of energy
MDO	Multidisciplinary design optimisation
MMAEP	Mean mechanical annual energy production (of the array)
MMAEP_i	MMAEP for rotor i
NPC	Net present cost
OPEX	Operational expenditure
RVF	Representative velocity field
TEC	Tidal energy converter
UH-CMA-ES	Uncertainly handling covariance matrix adaptation evolution strategy
UTM	Universal Transverse Mercator

a 10 MW array is predicted by [8] to have an LCOE of approximately \$400/MW h, whereas diesel generation is estimated to be within the \$200 – \$300/MW h range [9].

Techno-economic modelling of electricity generation plant parametrises technical design choices and calculates the impact of those choices on both plant cost and lifetime energy production. This allows such modelling to be used to investigate ways of reducing the LCOE of individual plants and the technology as a whole; for instance, the optimal power rating of wave energy converters was calculated in [10]. Techno-economic models incorporate multiple social science, physical and engineering disciplines; the study of solving such problems is known as multidisciplinary design optimisation (MDO) [11]. Different approaches can be taken to tackle MDO problems, such as the 'traditional' approach, where each discipline is optimised in turn [12] or the contemporary 'global' approach, where all disciplines are optimised in unison. A contemporary MDO approach to the optimisation of offshore wind farms was demonstrated in [13].

The effects of tidal energy conversion on the resource are well understood [14–17], yet assumptions are often made in relation to other techno-economic aspects, in order to reduce complexity. For instance, it is commonly assumed that TEC arrays should be designed to maximise power extraction (see e.g. [18, chap. 5]). Yet, in [19,20] it was shown that such arrays are not optimal when considering environmental impact, while [5] shows that, for a large artificial array, the maximum profit layout did not produce the most power. This assumption is related to the choice of the longitudinal (row) spacing of TEC arrays, where 20 rotor diameters (see [21]) has become the default, with this value being applied in studies such as [8], for example. The implicit assumption here is that minimising negative TEC interactions maximises economic efficiency.

This work examines if the assumptions identified above are valid for small[1] area-constrained arrays by developing a novel analytical model of LCOE with respect to annual energy production. The model assumes that costs scale linearly with the number of TECs deployed, and captures the energy lost to interactions as TECs are added to an optimally positioned array. To verify the axioms of the model, comparison is made to a numerical model free of such assumptions. In [22], application of the state-of-the-art open-source techno-economic wave and tidal energy array modelling tool 'DTOcean'[2] to hypothetical TEC

[1] [17] describes a small array as "one too small to influence channel-scale dynamics".

[2] DTOcean can be downloaded from github.com/dtocean.

arrays in the Tacoma Narrows, USA, was demonstrated. DTOcean can model TEC array power production, including the interaction between TECs; design and cost the electrical network, moorings and foundations; determine the installation requirements; and calculate the associated lifetime operational expenditure and energy production. This provides unique insight into the influence of these individual cost factors on the design and economics of an array.

The utility of the DTOcean methodology is evidenced by previous studies. In [22,23] DTOcean was used to recreate the semi-analytical techno-economic models developed in the US Department of Energy's 'Reference Model Project' [8] for both wave (RM3) and tidal arrays (RM1), respectively. The intention of DTOcean is not to verify an absolute value of LCOE, but to provide a standardised methodology and discover more efficient array designs by assessing the impact of change. Thus, in the aforementioned studies interesting scale effects were witnessed which were not predicted by the semi-analytical approach, while a number of assumptions were shown to not be technically feasible. DTOcean has also revealed fundamental aspects of LCOE prediction for ocean energy arrays, in particular that the LCOE should not be treated as a singular value, but as a statistical distribution that is influenced by the decisions of the designer [23].

To compare the DTOcean results with the analytical model, the optimisation approach of DTOcean was advanced within this work, by removing the assumption that TEC arrays should be laid out to maximise power and adding a global optimisation architecture where LCOE determines TEC positions. This elevates DTOcean beyond the existing numerical methods for optimisation of the LCOE of TEC arrays. Although micro-siting of TEC devices in techno-economic arrays has previously been demonstrated using gradient based methods [16], heuristic algorithms [24], and surrogate modelling of computational fluid dynamics (CFD) solutions [25], all of these studies rely on simplistic estimates for the balance-of-plant subsystems which affect cost and array availability. The DTOcean approach, as demonstrated in this work, combines freedom of device positioning, with detailed balance-of-plant modelling.

Once verified, the analytical LCOE model predicts the level of interaction between TECs that is most economical — a meaningful step forward in understanding economic optimality of small TEC arrays. Previously, the relationship of LCOE to the number of devices in an array (a proxy for energy production, in this case) was presented by [26, sec. 10.1], but their analysis did not consider interactions between devices. The relationship of array LCOE with energy lost to interactions is addressed in [27], but only a single array with fixed configuration is considered. Our analytical LCOE model considers all possible array sizes, where each array is optimally positioned. Significantly, where [27] concludes that negative interactions are detrimental to the LCOE of tidal energy arrays, the model proposed herein offers an alternative perspective, i.e. that given a fixed deployment area, allowing interactions can (conditionally) offer significant improvements in LCOE.

The outline of this article is as follows. Section 2.1, provides an introduction to techno-economic modelling of TEC arrays. In Section 2.2, the hypothetical model of LCOE to energy production for small arrays is developed. Section 2.3 introduces the DTOcean software, while the theoretical and numerical implementation of an updated optimisation architecture for DTOcean is given in Section 2.4. Subsequently, an experiment to test the hypothetical LCOE model, using the new architecture, is described in Section 2.5. The results of the experiment are then presented in Section 3, discussed in Section 4, before concluding remarks are given in Section 5.

2. Method

2.1. Techno-economic tidal energy converter array modelling

Given the selection of a suitable deployment site, it is convenient to subdivide the design and operation of an array of TECs within the site into stages, including:

- The TEC design
- Locating the TECs and calculating the energy extracted
- Design of the electrical network to transport the captured energy to shore
- Design of the station keeping requirements of the TECs and other infrastructure
- Calculating the costs and time elapsed for installation operations
- Calculating the costs and energy lost due to maintenance of the array
- Calculating the costs of decommissioning

The decommissioning stage is often disregarded, as many of the metrics of interest are discounted (i.e. given in their present value, subject to some discount rate), thus costs incurred at the end of a (long) project lifetime have little influence. Whether the TEC design is included in an array model often relates to the maturity of the technology, with less mature technologies, possibly with technology readiness level (TRL) less than 7 [28], being designed as part of the model and more mature technologies being considered to have a fixed design.

Techno-economic models must provide a means to evaluate the economic efficiency of a deployment. LCOE is an excellent metric for amalgamating the complex energy and cost factors involved in TEC array design into a single value. Often LCOE is used to compare different energy generation technologies (see e.g. [29]); however, the metric can also be used for comparison of relative array configurations (the uncertainty surrounding the absolute value can be high given the level of assumption, for example, in component costs and reliability values). The LCOE can be summarised as:

$$\mathrm{LCOE} = \frac{c^0 + \mathrm{NPC}(\mathbf{C})}{\mathrm{NPC}(\mathbf{E})} \tag{1}$$

where c^0 are costs incurred prior to commencement of the project (at year zero); $\mathbf{C}$ and $\mathbf{E}$ are the costs incurred and energy exported, respectively, for each year of operation; and NPC is the net present cost function, given by

$$\mathrm{NPC}(\mathbf{x}) = \sum_{i=1}^{n_t} \frac{x_i}{(1+d)^i} \tag{2}$$

where n_t is the number of years in the project and d is the discount rate.

Other non-numerical metrics are also important to the design of TEC arrays, such as the environmental impact. As the topic of this paper concerns hypothetical techno-economic optimisation of TEC arrays, the environmental impact is not considered here, but certain important aspects related to the results of the article are discussed in Section 4. Although outside of the scope of this work, understanding local environmental impacts and wider social costs and benefits are vital for real deployments.

2.2. Hypothetical relationship of LCOE to energy production

An analytical model to describe the relationship of LCOE to mean mechanical annual energy production (MMAEP) (the annual energy production without losses due to transmission or maintenance downtime) for a small, area-constrained, tidal energy converter arrays is developed within this section. The model provides a theoretical framework for examining the relationship between device interactions and economic efficiency.

It is assumed that costs scale linearly with the number of TECs deployed, and interactions between TECs are assumed only to affect the energy production of the array. Under these assumptions, and the assumption that the number of TECs, n_x, is continuous, the year zero array cost is written

$$c^0(n_x) = c_0 + n_x c_x, \tag{3}$$

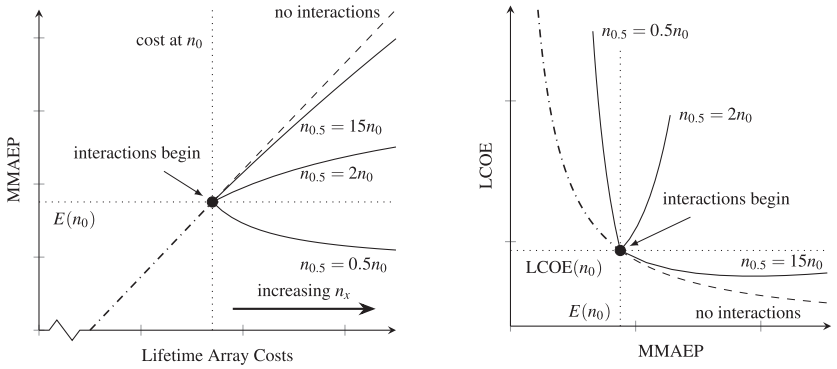

Fig. 1. Examples of solution class behaviours for the hypothetical LCOE model. The relationship of MMAEP to lifetime array cost is shown in (a) and the relationship of LCOE to MMAEP is shown in (b). The dot-dashed line indicates the values prior to device interaction, the solid lines indicate alternative behaviours based on the value of $n_{0.5}$, and the behaviour if no interactions were to occur is shown by the dashed line.

where c_0 are constant costs and c_x is the additional cost per TEC. The annual costs, for year i, are given as

$$c^i(n_x) = c_e + n_x c_m, \tag{4}$$

where c_m is the maintenance cost per TEC and c_e are any additional fixed annual costs, such as for environmental monitoring. This formulation requires that installation is instantaneous (i.e. it can be included in Eq. (3)) and that maintenance of array level subsystems, such as the export cable, is negligible. Where no interactions are present between TECs in the array, the MMAEP of the array (in watt-hours) is

$$E(n_x) = C_{\text{cap}} P_{\text{rated}} T_a n_x \tag{5}$$

where C_{cap} is the array capacity factor, P_{rated} is the rated power of the TEC and T_a is the number of hours in a year.

By design, costs are assumed invariant per year of operation of the array. In addition, by assuming that energy losses from downtime are negligible, the array energy production can be treated similarly. For constant annual input, the net present cost function, given by Eq. (2), can be treated as the sum of a finite geometric series. Letting $\hat{d} = (1+d)^{-1}$ and letting x be the constant input for all years, Eq. (2) becomes

$$\text{NPC}(x) = \sum_{i=1}^{n_t} x\hat{d}^i = x\hat{d}\left(\frac{1-\hat{d}^{n_t}}{1-\hat{d}}\right).$$

Subsequently, by defining

$$C_d = \hat{d}\left(\frac{1-\hat{d}^{n_t}}{1-\hat{d}}\right),$$

the NPC for constant annual input is

$$\text{NPC}(x) = C_d x. \tag{6}$$

An expression for the LCOE can now be derived by substituting Eqs. (3), (4) and (5) into Eq. (1), utilising the constant NPC expression given by Eq. (6). Collecting powers of n_x, this gives

$$\text{LCOE} = \frac{c_n n_x + c_f}{C_d C_{\text{cap}} P_{\text{rated}} T_a n_x}, \quad n_x < n_0, \tag{7}$$

where n_0 is the number of TECs after which interactions begin to affect energy production,[3] $c_f = c_0 + C_d c_e$ and $c_n = c_x + C_d c_m$.

When sufficient TECs are added to the array such that negative interactions occur ($n_x > n_0$), the total MMAEP of the array will reduce. To model this phenomenon, a multiplier ($g(n_x)$) is applied to the undisturbed MMAEP of an array of size n_x, such that

$$E(n_x) = g(n_x) C_{\text{cap}} P_{\text{rated}} T_a n_x,$$

where g is a general reciprocal function given by

$$g(x) = \frac{a}{b+x},$$

with constants a, b to be determined. By continuity, $g(n_0) = 1$ and if the value of g is assumed to halve after an additional $n_{0.5}$ TECs are added to the array,[4] i.e. $g(n_0 + n_{0.5}) = 0.5$, then

$$g(n_x) = \frac{n_{0.5}}{n_x + n_{0.5} - n_0}.$$

Under the same assumptions as Eq. (7), the LCOE is now given as

$$\text{LCOE} = \frac{c_n n_x^2 + (c_f + c_n n_{0.5} - c_n n_0) n_x + c_f (n_{0.5} - n_0)}{n_{0.5} C_d C_{\text{cap}} P_{\text{rated}} T_a n_x}, \quad n_x \geq n_0. \tag{8}$$

Physically, the $n_{0.5}$ parameter controls the rate of energy lost to hydrodynamic interactions as more TECs are added to an array. Depending on the value of $n_{0.5}$, Eq. (8) exhibits three 'classes' of solution, which represent different behaviours for MMAEP and LCOE as more TECs are added to the array. These behaviours are classified as follows:

- For $n_{0.5} <= n_0$, the array MMAEP reduces (or remains constant) as more TECs are added and the LCOE increases.
- For $n_{0.5} > n_0$, the array MMAEP increases as more TECs are added while the LCOE also increases.
- Finally, for some $n_{0.5} \gg n_0$, the array MMAEP increases as more TECs are added but the LCOE initially decreases to some minimum before increasing.

In Fig. 1, these concepts are demonstrated by considering how a solution from each class evolves for MMAEP with respect to lifetime array costs (Fig. 1(a)) and LCOE with respect to MMAEP (Fig. 1(b)). Initially, lifetime array costs increase with the number of TECs and MMAEP increases proportionately (indicated by the dot-dashed line in Fig. 1(a)) until more than n_0 TECs are deployed (after which negative interactions occur). Subsequently, depending on the value of $n_{0.5}$, different behaviours are observed when additional TECs are added, illustrated by the solid lines to the right of the vertical dashed line

[3] Although certain array orientations can generate positive hydrodynamic interactions between TECs, the interactions considered here are the net negative energy loss from all TECS in an array.

[4] Note that $n_{0.5}$ does not set the number of TECs at which the MMAEP of the array is halved relative to the MMAEP for n_0 TECs. It describes the additional number of TECs required for the MMAEP of *all* TECs in the array subject to interaction ($E(n_0 + n_{0.5})$) to be half of the value if no interactions occurred for the same number of TECs.

Table 1
Ocean energy converter (OEC) array simulation scope and modelling assumptions for the DTOcean software. Adapted from [23].

OEC types	Fixed-design floating or bottom fixed wave or tidal
Mixed OEC type	Single type per simulation
Maximum number of OECs	100
Maximum deployment depths	80 m for tidal, 200 m for wave
Sedimentary layers	Single or multi-layered strata
Electrical network types	Single substation, single export cable
Foundation types	Gravity, piles, anchors, suction caissons, shallow
Mooring types	Catenary or taut
Logistics	Single port, one vessel per operation
Maintenance strategies	Corrective, calendar- or condition-based
Decommissioning	Not included

indicating the array costs at n_0 TECs, in Fig. 1(a). The $n_{0.5} = 0.5n_0$ line is an example of the $n_{0.5} <= n_0$ class, defined by solutions where MMAEP reduces as lifetime costs increase (i.e. as more TECs are added, the mechanical energy of the array must reduce). The $n_{0.5} = 2n_0$ and $n_{0.5} = 15n_0$ lines are examples of the $n_{0.5} > n_0$ and $n_{0.5} \gg n_0$ solution classes, respectively. For both of these classes MMAEP increases with lifetime array costs. These two classes are differentiated by examining the relationship of LCOE to MMAEP as shown in Fig. 1(b). Similarly to Fig. 1(a), the solution prior to TEC interactions is shown by the dot-dashed line to the left of the vertical dashed line; the horizontal dashed line indicates the LCOE value at n_0 TECs. Here, the behaviour of the $n_{0.5} > n_0$ solutions are discerned from the $n_{0.5} \gg n_0$ solutions by the LCOE response as the array MMAEP increases. As shown by the $n_{0.5} = 2n_0$ example line, the $n_{0.5} > n_0$ class of solutions is identified by increasing LCOE with additional MMAEP, while the $n_{0.5} \gg n_0$ class, shown by the $n_{0.5} = 15n_0$ line, is identified by LCOE which reduces to some minimum before increasing again. For the $n_{0.5} <= n_0$ class, illustrated by the $n_{0.5} = 0.5n_0$ example, LCOE increases with additional TECs as MMAEP reduces or stays constant.

If the model described by Eqs. (7) and (8) correctly captures the key aggregate metrics of the optimally positioned arrays, then there exists solutions (e.g. for $n_{0.5} > n_0$ and $n_{0.5} \gg n_0$) where maximising the MMAEP of an array does not lead to minimum LCOE, contrary to the typical assumption otherwise. The remainder of this article is dedicated to testing the validity of the proposed model.

2.3. Numerical method

To test the hypothetical model developed in the preceding section, the techno-economic wave and tidal energy array modelling tool 'DTOcean' is applied. In the absence of real-world validation data, DTOcean is appropriate for this purpose as it is free from the linear cost assumption inherent to the hypothetical model. The scope and assumptions of DTOcean are shown in Table 1. DTOcean was originally designed for deployment of high TRL technologies, and so does not consider the TEC design as part of the array model. The software automates TEC array design using modules to represent the stages; the purpose of each module is shown in Table 2. This section provides an overview of the existing features that are pertinent to this work (new features are detailed in the next section). For further details, a comprehensive description of tidal hydrodynamics solver used by DTOcean is available in [22], while the mechanics of the remaining modules are described in [23].

DTOcean solves the interactions between TECs using a modification of the 'Jensen' model [30], which superimposes wakes of upstream turbines to calculate deficits at downstream turbines. DTOcean's method advances this concept by modelling the wakes using a detailed CFD simulations of a non-dimensional reference turbine, and applying the wakes along the streamlines of the flow, rather than perpendicular to the rotor disc. To reduce simulation time, the tidal cycles are broken down into a limited number of 'representative velocity fields' (RVFs), where a flow field is associated with a probability of occurrence.

Table 2
Description of modules provided by the DTOcean software. Adapted from [23].

Name	Purpose
Array Hydrodynamics	Locate TECs and calculate their power generation
Electrical Sub-Systems	Design an electrical network suited to the TEC and export cable characteristics and calculate losses
Moorings and Foundations	Design foundations and moorings (if appropriate) subject to array requirements and extreme conditions
Installation	Simulate the installation of all requested design phases
Maintenance	Simulate the maintenance activity over the array lifetime and record yearly costs and energy production

If $\mathbb{P}(\omega)$ ($\omega = 1, \ldots, n_s$ where n_s is the total number of RVFs) represent the probability of occurrence of each RVF, then the array MMAEP is given by

$$\text{MMAEP} = \sum_{i}^{n_r} \text{MMAEP}_i \qquad \text{where}$$

$$\text{MMAEP}_i = T_a \sum_{\omega}^{n_s} P_i(\omega)\mathbb{P}(\omega).$$

Here, n_r is the number of rotors in the array, MMAEP_i is the MMAEP (in units of watt-hours) for TEC rotor i and $P_i(\omega)$ is the power production of rotor i for velocity field ω.

A metric which measures the interactions between TECs is also useful when comparing simulations. The metric used herein, known as the 'q-factor', measures the ratio of power production with and without interactions. If the undisturbed power production for each rotor is given by P_i^0, then

$$\mathbb{q}_i = \frac{\sum_{\omega}^{n_s} P_i(\omega)}{\sum_{\omega}^{n_s} P_i^0(\omega)},$$

$$\mathbb{q} = \frac{\sum_{i}^{n_r}\sum_{\omega}^{n_s} P_i(\omega)}{\sum_{i}^{n_r}\sum_{\omega}^{n_s} P_i^0(\omega)},$$

where $\mathbb{q}_i$ and $\mathbb{q}$ are the q-factors for rotor i and the array, respectively.

The electrical network, moorings and foundations of the array are designed by component, forming large networks to represent the higher-level subsystems which can change dynamically depending on the configuration of the array. This provides detailed estimates of the costs and reliability of the high-level subsystems. Additionally, a power flow model [31] is used to calculate the efficiency of the electrical network. The logistics for the installation and maintenance phases are modelled in the time-domain, providing realistic estimates for the cost and duration of such operations, subject to environmental conditions. Modelled random failures of the TEC and balance-of-plant subsystems are combined with varying environmental conditions to provide a novel statistical representation of downtime and maintenance costs. As described in [23], the variability modelled in the costs and energy production due to the array maintenance renders the LCOE a statistical quantity, also.

DTOcean's approach to solving the hydrodynamic interactions of the TECs has advantages and disadvantages compared to other numerical schemes. As noted in [22], although models based on the shallow water equations, such as [16,19], provide an efficient means of simulating large arrays of TECs, the predicted recovery of the TEC's wakes may not be accurate [32,33]. Alternatively, accurate wake evolution can be modelled using CFD but at high computational cost [34]. By combining a pre-computed CFD wake model with a fast superposition method, the DTOcean approach is sufficiently rapid to allow inclusion of detailed balance-of-plants models, while accurately predicting TEC wake recovery. A disadvantage of the DTOcean approach is that the undisturbed flow is not modified. Therefore, if an array large enough

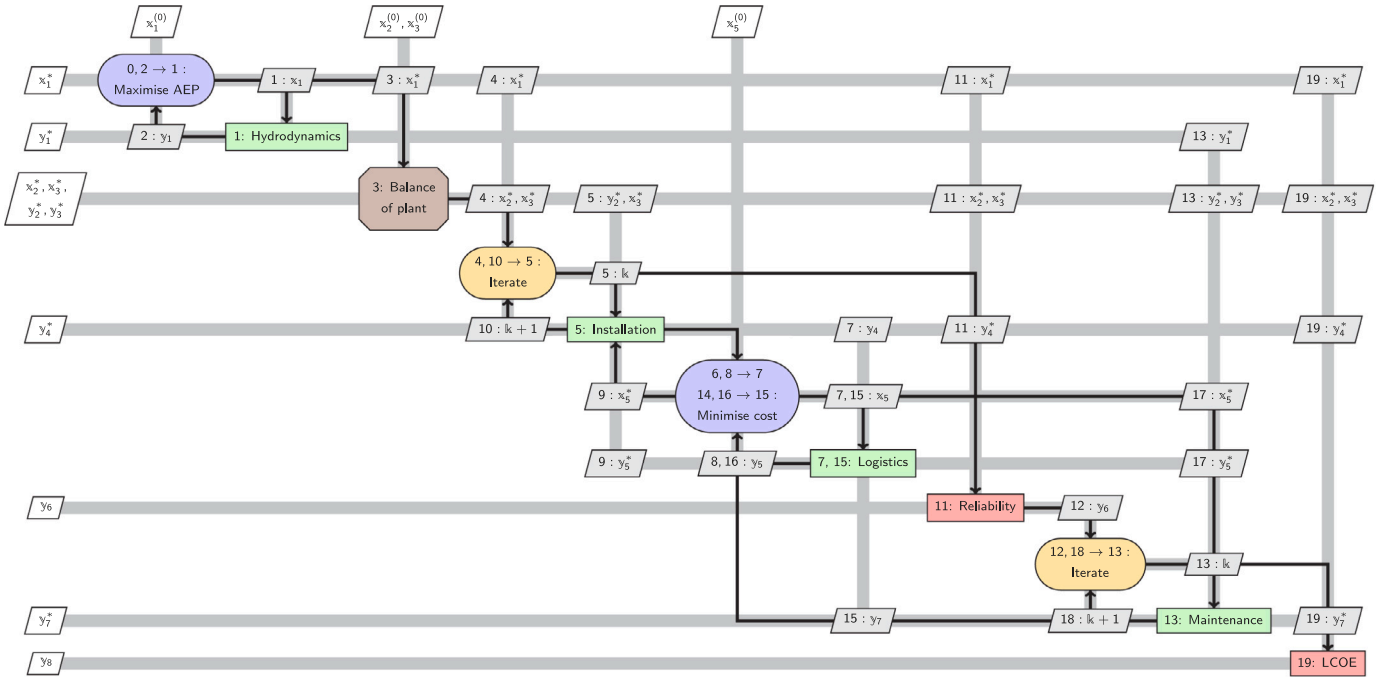

Fig. 2. XDSM diagram of the original DTOcean's sequential optimisation process. See Fig. 3 for the full balance of plant stage (step 3) and Table 3 for examples of variables transferred.

to affect the channel resource is simulated, the energy production predicted by DTOcean would be overestimated. For this reason, the arrays simulated herein are considered 'small' by the definition of [17]. In lower blockage scenarios the reference velocity fields that DTOcean relies on will be less affected at the channel scale, which is corroborated by the results of [19], for instance.

2.4. Optimisation

The original MDO architecture of DTOcean assumed that the number of TECs which maximised the MMAEP of an array also minimised the LCOE. In order to examine the influence of the number of TECs on the LCOE of the array, a new global MDO architecture is added to DTOcean. (With this goal in mind, the reader may move onto Section 2.5 without loss of understanding of the overall article.) This section introduces the general optimisation problem, the original MDO approach of DTOcean, and the updated architecture used within this study.

Letting $\mathbb{x}$ refer to design variables and $\mathbb{y}$ to coupling and state variables (i.e. outputs of analyses), following the nomenclature defined by [11], Eq. (1) becomes

$$f(\mathbb{x},\mathbb{y}) = \frac{c^0(\mathbb{x}) + \mathrm{NPC}(\mathbf{C}(\mathbb{x},\mathbb{y}(\mathbb{x},\mathbb{y})))}{\mathrm{NPC}(\mathbf{E}(\mathbb{x},\mathbb{y}(\mathbb{x},\mathbb{y})))}. \tag{9}$$

Subsequently, the related optimisation problem can be stated as

$$\begin{aligned} \underset{\mathbb{x},\mathbb{y}}{\text{minimise}} \quad & f(\mathbb{x},\mathbb{y}) \\ \text{subject to} \quad & \mathbb{c}_0(\mathbb{x},\mathbb{y}) \geq 0, \\ & \mathbb{c}_i(\mathbb{x}_0,\mathbb{x}_i,\mathbb{y}_i) \geq 0, \\ & \mathcal{R}(\mathbb{x}_0,\mathbb{x}_i,\mathbb{y}_j \neq \mathbb{y}_i,\mathbb{y}_i) = 0 \end{aligned} \tag{10}$$

where $\mathbb{c}$ are constraints and $\mathcal{R}$ refers to the residual form of each discipline's governing equations. The subscript '0' implies functions or variables shared by more than one discipline, and 'i' or 'j' refer to functions or variables for a single discipline. Note, $\mathbb{c}_0$ and $\mathbb{c}_i$ are a generalisation of the true constraints of the problem, used here for illustration.

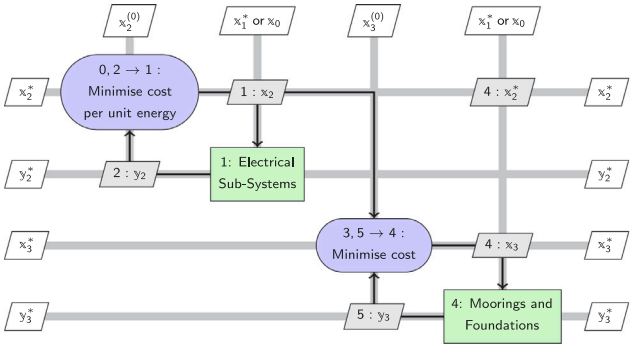

Fig. 3. XDSM diagram of the balance-of-plant optimisation stages. See Table 3 for examples of variables transferred.

2.4.1. Traditional MDO approach

The original architecture of the DTOcean tool follows a 'traditional MDO approach' [12], where Eq. (10) is decomposed into a number of smaller optimisation problems, divided along disciplinary lines, which are solved sequentially. Figs. 2 and 3 show extended design structure matrix (XDSM) diagrams of this architecture. As defined in [11], 'components' in an XDSM diagram are laid out along the diagonal, which consist of discipline analyses and functions (straight edged rectangles), and 'drivers' which control process flow (rounded rectangles). Here, the discipline analyses are split into the design components (in green) and functions that provide metrics based on the calculated designs (in red). Two types of drivers are shown, one to represent an optimisation process (in blue) and another (in yellow) to show a basic iteration (over index '$\mathbb{k}$'). The brown chamfered rectangle indicates that the components have been abbreviated, in this case for the balance-of-plant calculations shown in Fig. 3. The data flow is shown as thick grey lines, and components take data inputs from the vertical direction and output data in the horizontal direction. The off-diagonal nodes in the shape of parallelograms are used to label the data transferred between components. External inputs are provided from the top and returned as outputs to the left. Data with an asterisk superscript represents final values. The thin black lines show the process flow and a numbering

Table 3
Optimisation problem statements, per discipline, for the decomposed LCOE optimisation problem, as developed in the original DTOcean tool. See also Figs. 2 and 3.

Discipline	Problem statement	Objective function	Noteworthy variables
Hydrodynamics	$\mathbb{y}_1^* = \max_{\mathbb{x}_1} f_1(\mathbb{x}_1)$	Mechanical energy production	Energy and TEC quantities and positions
Electrical Sub-Systems	$\mathbb{y}_2^* = \min_{\mathbb{x}_2} f_2(\mathbb{x}_1^*, \mathbb{x}_2, \mathbb{y}_1^*)$	Cost per unit energy transmitted	Components and transmission losses
Moorings and Foundations	$\mathbb{y}_3^* = \min_{\mathbb{x}_3} f_3(\mathbb{x}_1^*, \mathbb{x}_2^*, \mathbb{x}_3)$	Cost	Components
Installation	$\mathbb{y}_4^* = \min_{\mathbb{x}_5} f_4(\mathbb{x}_1^*, \mathbb{x}_2^*, \mathbb{x}_3^*, \mathbb{x}_5, \mathbb{y}_2^*, \mathbb{y}_3^*)$	Logistics costs (installation)	Installation schedule and costs
Maintenance	$\mathbb{y}_7^* = \min_{\mathbb{x}_5} f_5(\mathbb{x}_1^*, \mathbb{x}_2^*, \mathbb{x}_3^*, \mathbb{x}_5, \mathbb{y}_1^*, \mathbb{y}_2^*, \mathbb{y}_3^*, \mathbb{y}_4^*)$	Logistics costs (operations)	Lifetime energy and maintenance costs

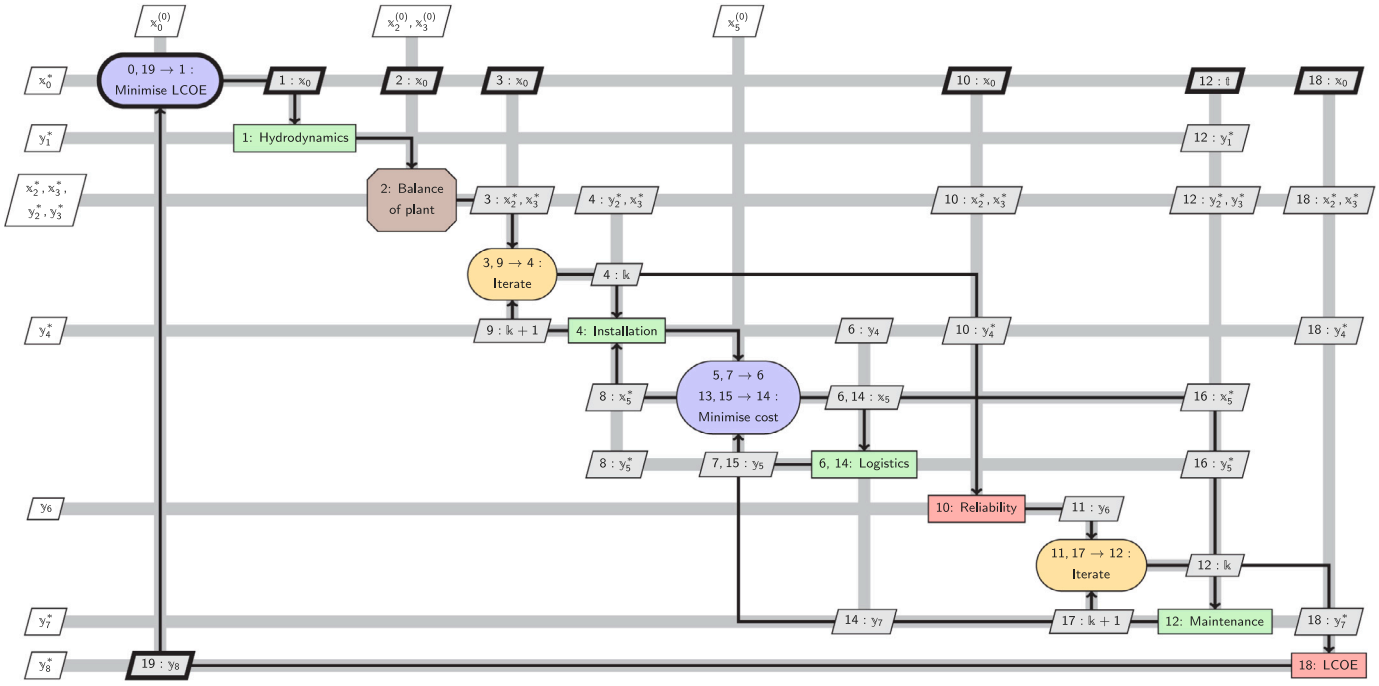

Fig. 4. XDSM diagram of the novel global optimisation process, with significant changes to the original architecture shown by bold outlines. Observe the global optimisation block (step 0) and the passing of the global optimisation variable, $\mathbb{x}_0$. Feedback of the LCOE to the global optimiser is shown by step 19. Also note the parameter $\mathbb{t}$ which controls the accuracy of the solution generated by the maintenance module (in step 12). See Fig. 3 for the full balance of plant stage (step 2) and Table 3 for examples of variables transferred.

system is used to show the order in which the components are executed (presented inside the nodes of the diagram followed by a colon). Loops are denoted by $i \rightarrow j$, indicating that the algorithm must return to step j until some condition is satisfied. The objective function of optimisation drivers is shown, and the name of the discipline or function is provided in the other component nodes.

The specific details of the drivers $\mathbb{x}_1, \ldots \mathbb{x}_5$ and coupling variables $\mathbb{y}_1, \ldots, \mathbb{y}_7$ are not included here for brevity, however a number of noteworthy variables for each discipline are given in Table 3, which also shows a summary of the individual problem statements. Note that there is no feedback of coupling variables to disciplines executed earlier in the process flow, which was a deliberate choice of the original DTOcean design, to reduce the difficulty of the interdisciplinary coupling problem, and improve computational efficiency.

Under this architecture, and using the nomenclature defined in Table 3, Eq. (9) becomes

$$\mathbb{y}_8 = \frac{c^0(\mathbb{x}_1^* + \mathbb{x}_2^* + \mathbb{x}_3^*) + \mathrm{NPC}(\mathbf{C}(\mathbb{y}_4^* + \mathbb{y}_7^*))}{\mathrm{NPC}(\mathbf{E}(\mathbb{y}_7^*))}. \tag{11}$$

where $\mathbb{y}_8$ is the LCOE. Eq. (11) in combination with Table 3 shows the limitations of this architecture as an approximation to the optimisation problem given by Eqs. (9) and (10). One issue is that the operations and maintenance term, $\mathbb{y}_7^*$, appears on both the top and bottom of the equation, and is also a function of all the other terms. Additionally, both this term, and the term relating to installation, $\mathbb{y}_4^*$, are optimised per logistics operation. Thus, the temporal element of the optimisation problem, due to the NPC function, is ignored.

Another significant problem with the original DTOcean approach is the effect of the hydrodynamics optimisation on Eq. (11). The objective is to generate as much mechanical energy as possible, yet this may, under certain circumstances such as in area-constrained arrays, only add marginal gains to the $\mathbb{y}_7^*$ in the denominator, while increasing the value of all terms in the numerator. As noted in [35], this issue was anticipated in the optimisation problem of the hydrodynamics module and an arbitrary constraint on the q-factor was added to the problem statement, "to prevent the array layout solution from overfilling". As seen in the next subsection, the local optimisation within the hydrodynamics module is removed, eliminating the need for this additional constraint.

2.4.2. Updated optimisation architecture

This work makes the first attempt to reformulate the DTOcean optimisation approach as a contemporary MDO problem. To achieve this, the optimisation problem for the hydrodynamics module, f_1 is removed, and a global optimisation loop is added as shown in Fig. 4. Additionally, all of the $\mathbb{x}_1^*$ terms in the remaining optimisation problems in Table 3 are replaced by the global optimisation design variable, $\mathbb{x}_0$.

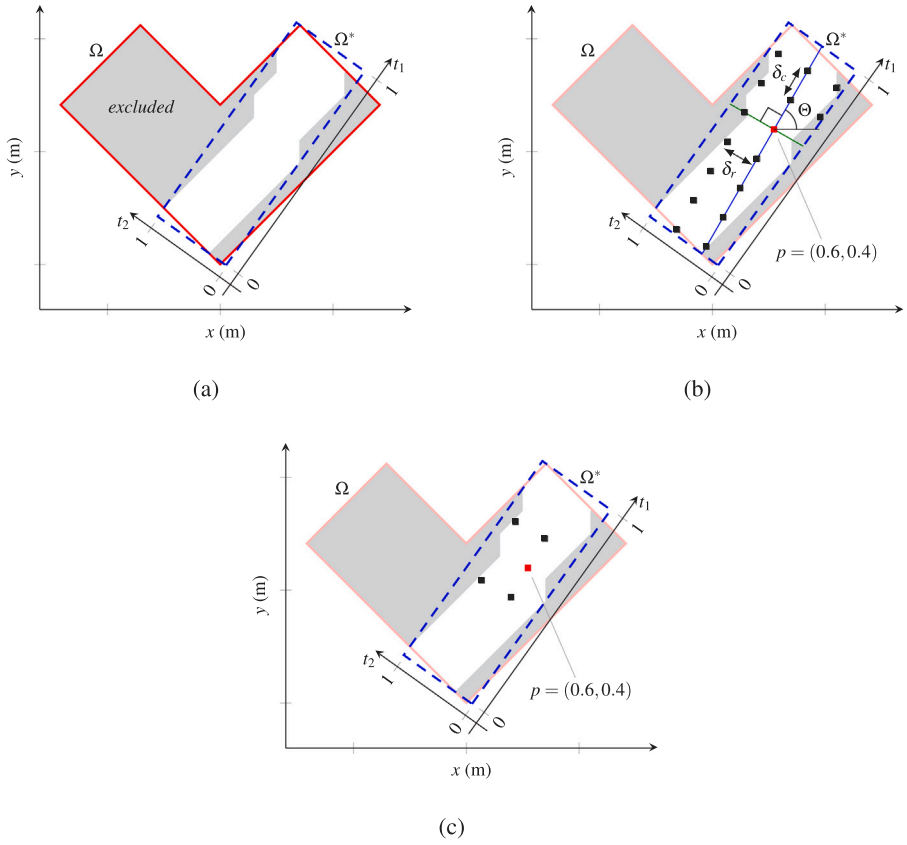

Fig. 5. The TEC position selection process. Following exclusion of invalid regions in the domain of Ω, due to bathymetric or other constraints, a parametric space (t_1, t_2) is fitted to the minimum-area enclosing rectangle (Ω^*) of the remaining, valid, area, as shown in (a). A regular grid of nodes, centred at $p(t_1, t_2)$, is generated within Ω^* with row spacing δ_r and column spacing δ_c, and rotated by Θ, as shown in (b) for $p = (0.6, 0.4)$. Finally, the n_x nodes closest to p that do not violate the constraints are chosen, with an array of five nodes shown in (c).

Defining the new global objective function as

$$f_0 = \frac{c^0(\mathbb{x}_0 + \mathbb{x}_2^* + \mathbb{x}_3^*) + \mathrm{NPC}(\mathbf{C}(\mathbb{y}_4^* + \mathbb{y}_7^*))}{\mathrm{NPC}(\mathbf{E}(\mathbb{y}_7^*))},$$

the global optimisation problem is

$$\begin{aligned} \underset{\mathbb{x}_0}{\text{minimise}} \quad & f_0 \qquad \text{where } \mathbb{x}_0 = (\mathbf{x}_1, \ldots, \mathbf{x}_{n_x}) \\ \text{subject to} \quad & \#\mathbf{x} = n_x, \\ & \left\|\mathbf{x}_i - \mathbf{x}_j\right\| \geq r \quad i \neq j = 1, .., n_x, \\ & \mathbf{x}_i \in \Omega i = 1, \ldots, n_x, \\ & z^- \leq x_z \leq z^+ \end{aligned} \tag{12}$$

where # represents cardinality, n_x is the number of TECs, with positions $\mathbf{x}_i (i = 1, \ldots, n_x)$, to be optimised, Ω represents the deployment area for the TECs, r is the minimum spacing between TECs, and (z^-, z^+) are the limits on the vertical position of any TEC, x_z.

A number of other constraints exist within the local optimisation problems governed by f_2, f_3, f_4, f_5, that may be violated by the TEC positions selected through the optimisation of f_0. These include the inability to design a valid electrical infrastructure or the inability to provide an adequate station keeping solution due to the local geology about a particular TEC. For brevity, the mathematical description of all the remaining constraints is omitted from this text; however, further information can be found in [23,36] or the DTOcean project deliverables (available from [37]).

2.4.3. Numerical implementation

To generate a set of TEC positions, subject to the constraints listed in Eq. (12), a process based on that of [35] is applied which selects nodes from a parametrically defined 'positioning' grid placed atop the computational domain, Ω, as illustrated by Fig. 5. The process improves upon [35] by allowing TECs to be placed within the domain with fixed spacing, centred at an arbitrary position. Previously, the TECs were always evenly distributed across the domain, leading to very large distances between TECs for small deployments. Within this work, no grid skewing (allowing angles between the grid rows and columns not equal to 90 degrees) is used, in order to reduce computational complexity.

The TEC positioning process redefines the optimisation problem given by Eq. (12) with respect to the variables δ_r, δ_c, Θ, p_1 and p_2, where δ_r and δ_c are the positioning grid row and column spacing, respectively, Θ is the grid rotation angle, and p_1 and p_2 are the coordinates of the 'central point' within the parametric space (as defined in Fig. 5) from which the nearest n_x grid nodes provide the TEC positions, $\mathbf{x}$. For a given n_x, values of these variables are generated by the heuristic UH-CMA-ES optimisation algorithm, described in Appendix A. The positioning algorithm automatically satisfies the minimum distance, area and depth constraints in Eq. (12), but has the potential to invalidate the cardinality constraint on $\mathbf{x}$, due to insufficient valid nodes being available. Following [38], the solutions in any given iteration are resampled until a population is found which does not violate any constraints. In the event that resampling fails to produce a valid population, a penalty value is returned for a new set of sampled solutions, calculated by

$$f_p = f_{\max} + \left\|\mathbb{x} - \mathbb{x}_{\text{feasible}}\right\|$$

where $f_{\max}$ is a user-provided value that should exceed the maximum expected value of f_0 and $\mathbb{x}_{\text{feasible}}$ is a feasible solution, chosen as the current best solution on first invocation of the penalty function. A maximum limit for the number of resample loops is set, sufficient to generate the initial population samples.

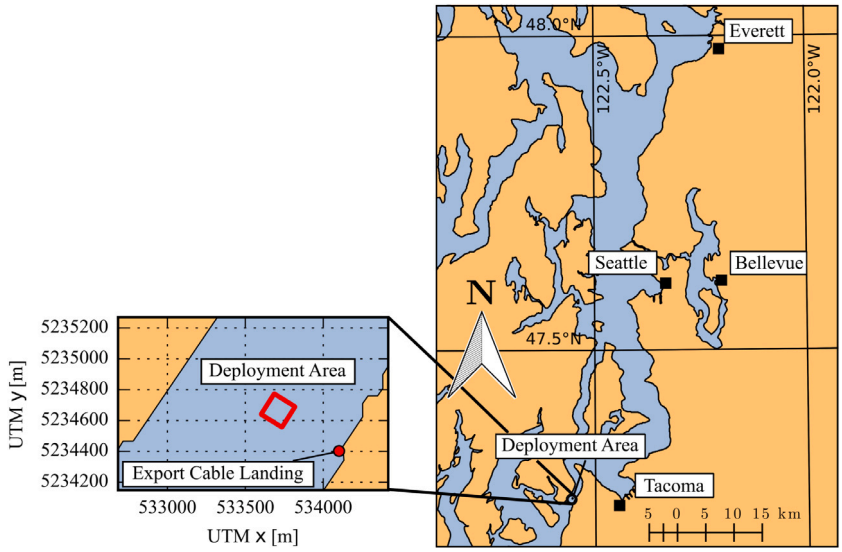

Fig. 6. Location of optimisation study deployment area within the Tacoma Narrows, in the U.S. state of Washington, relative to nearby medium and large cities.

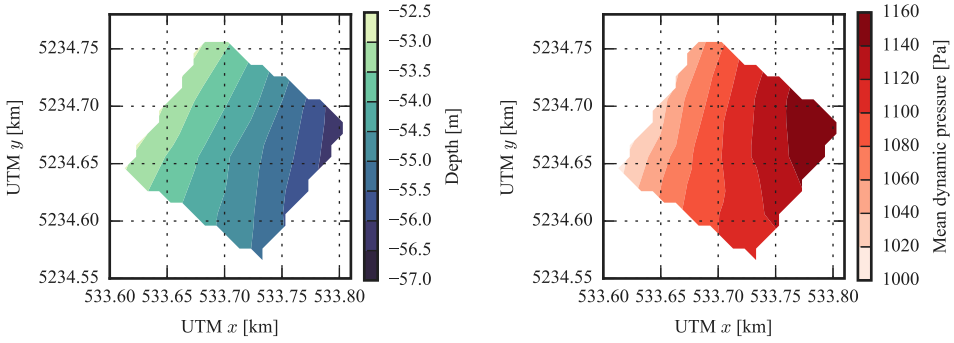

Fig. 7. Bathymetry (a) and mean dynamic pressure (b) for the optimisation study deployment area.

2.5. Experiment

A verified DTOcean model of hypothetical TEC arrays in the Tacoma Narrows, Washington, U.S.A, as developed in [22], is used as a baseline to investigate the LCOE model derived in Section 2.2. The Tacoma Narrows is an energetic tidally driven channel with maximum current velocities of just over $3\,\mathrm{m\,s^{-1}}$. The location of the deployment area chosen for the optimisation study, relative to nearby infrastructure and population centres, is shown in Fig. 6. The deployment area for the optimisation study is a square domain, of 2 ha area, centred within the Tacoma Narrows and aligned with the mean flow direction. The bathymetry and mean dynamic pressure in the deployment area is shown in Fig. 7.

The TEC used in the optimisation study is the 'RM1 device', defined in [8, chap. 3]. The TEC has two rotors connected by a crossbeam, as seen in Fig. 8. The RM1 device has a rated power of 1.1 MW with two rotors per TEC resulting in 550 kW per rotor. The power take-off was designed with a cut-in velocity of $0.5\,\mathrm{m\,s^{-1}}$ and a cut-out velocity of $3\,\mathrm{m\,s^{-1}}$. The TEC's performance curves are shown in Fig. 9. The RM1 device is not capable of yawing, but can operate bi-directionally. As per [8], the RM1 device is serviced twice annually, using the deep water 'Port of Everett' as the base of operations.

Most parameters established for the arrays simulated within [22] are reused here, including calibrations for the electrical network, foundations, installation and maintenance operations. As such, the arrays simulated as part of this study should be representative of those defined in the RM1 reference model [8]. Noteworthy economic variables are the discount rate, which is set to 0.113 and the fixed capital and annual operational costs (referred to here as externalities) which amount to $€4.1 \times 10^7$ upfront capital costs and $€1.81 \times 10^6$ operational costs per annum. The operational lifetime of the array is twenty years.

For this study, the minimum distance between TECs is reduced to one rotor diameter (D) in the lateral and longitudinal directions (from $4.5D$ and $18.75D$, respectively, as defined in [22]). Thus, the 2 ha deployment area could theoretically support fourteen machines. Yet, as all TECs share a single orientation (of the mean flow direction), it is unlikely that fourteen TECs can be placed without impinging on each other. To map the solution space, an optimisation study is conducted for each $n_x = 2, 3, \ldots$ until layouts can no longer be found within a reasonable time limit.

For a given number of TECs (n_x), the optimisation algorithm developed in Section 2.4 is applied to the chosen lateral and longitudinal spacing (δ_c and δ_r), array centre point (p_1, and p_2) and rotation (Θ). The median LCOE is used as the objective function and the algorithm will terminate once the optimal solution has achieved an accuracy of $€1.0 \times 10^{-3}/\mathrm{kW\,h}$ (i.e. $\pm 0.1\,¢/\mathrm{kW\,h}$).

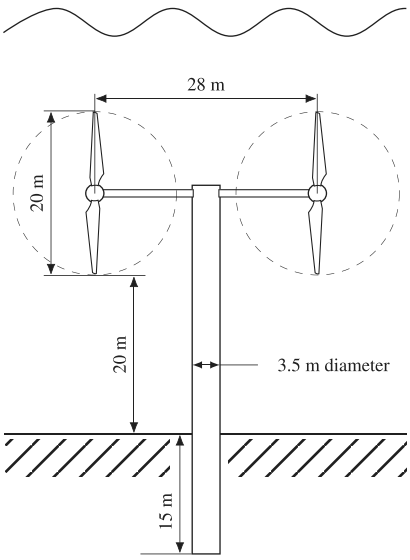

Fig. 8. RM1 device schematic.
Source: Reproduced from [8, 22].

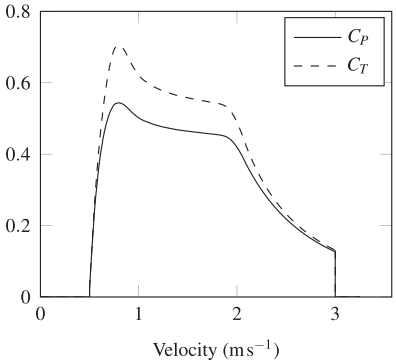

Fig. 9. Coefficients of power (C_P) and thrust (C_T), with respect to current velocity magnitude, for the RM1 device rotors.
Source: Reproduced from [22].

Table 4
Initial guess for design variables per optimisation study. The square brackets in the n_x column indicates a range. See nomenclature for variable definitions.

n_x	Θ (°)	δ_r (m)	δ_c (m)	p_1	p_2
[2, 3]	60.	25.	80.	0.5	0.5
4	0.	25.	80.	0.75	0.
[5, 8]	60.	25.	80.	0.5	0.5
9	30.	28.	67.	0.58	0.35
[10, 11]	60.	25.	80.	0.5	0.5
12	93.	24.5	53.5	0.326	0.362
13	60.	25.	80.	0.5	0.5

3. Results

The initial guesses for the design variables selected by the optimiser are given in Table 4. In certain circumstances some restarts of the UH-CMA-ES algorithm were required, if the algorithm failed to converge entirely or converged far from the minimum value solution. For $n_x = 12$, the range of Θ was restricted to [90, 95] degrees, in order to coerce the algorithm to converge near the minimum value evaluated. An optimisation study for a 14 TEC array was attempted, but insufficient viable layouts were discovered within a reasonable timescale.

The computational requirements of each optimisation study are shown in Table 5. The simulations were conducted using 4 GHz, 4-core, Intel i7-4790 and 4.1 GHz, 8-core, AMD 4750U CPUs. The maximum number of resamples that the optimiser required to find sufficient feasible solutions increased with array size. This made the wall-clock time of the early iterations extremely long for the larger array sizes; however, the number of resamples needed by the algorithm dropped to normal levels within a few iterations. The general trend was that more time and iterations were required to solve the optimisation problem as array sizes increased.

Table 5
Computational requirements for each optimisation study. 'Max resamples' refers to the maximum function evaluations required to complete the initial iterations, while the number of iterations, number of function evaluations, CPU type, number of threads used and wall-clock time required for convergence are also shown.

n_x	max resamples	iterations	evaluations	CPU	threads	time (h:m:s)
2	4	107	1189	i7-4790	6	9:50:52
3	11	149	1639	i7-4790	6	16:37:58
4	15	140	1488	i7-4790	6	15:49:44
5	35	134	1401	i7-4790	6	10:1:20
6	74	139	1482	i7-4790	6	25:25:13
7	136	126	1318	4750U	12	17:36:59
8	266	139	1482	4750U	12	25:24:21
9	661	136	1443	i7-4790	6	35:29:14
10	2488	129	1351	4750U	12	30:6:23
11	6402	77	769	i7-4790	6	29:56:0
12	83 571	127	1321	4750U	12	91:33:40
13	55 241	216	2297	i7-4790	6	146:43:28

Table 6
Median LCOE and solution values for the optimal layout for each optimisation study. See the nomenclature for variable definitions.

n_x	LCOE (€/kW h)	Θ (°)	δ_r(m)	δ_c(m)	p_1	p_2
2	0.9313	33.97	137.75	46.55	0.8297	0.0028
3	0.6621	179.23	76.76	27.39	0.8052	0.0283
4	0.5349	35.05	37.76	65.40	0.8065	0.0115
5	0.4677	31.10	32.18	66.17	0.9826	0.0085
6	0.4402	73.77	53.57	63.56	0.9859	0.3295
7	0.4150	127.58	56.78	39.87	0.0435	0.0029
8	0.3863	118.88	75.48	27.38	0.9994	0.8543
9	0.3766	0.06	63.72	28.15	0.0559	0.8383
10	0.3558	26.18	25.98	62.56	0.4214	0.5727
11	0.3511	91.07	61.43	24.45	0.5373	0.5538
12	0.3453	92.42	24.80	56.20	0.3931	0.3505
13	0.4218	42.39	23.76	56.95	0.2953	0.9315

The optimal solution and function value for each optimisation study is given in Table 6. It can be seen that an array of 12 TECs is found to have the lowest median LCOE. The array layouts of the optimal solutions for the 11, 12 and 13 TEC optimisation studies are shown in Fig. 10. Note the tendency for the optimiser to choose arrays that are staggered with respect to the oncoming flow and, also, the apparent proximity of some of the rotors in the array, a phenomenon which is discussed at greater length in Section 4.

A key assumption of the LCOE model presented in Section 2.2 was that the array costs scale linearly with the number of TECs in the array, as described by Eqs. (3) and (4). To verify this assumption, the correlation of the number of TECs with capital expenditure (CAPEX) and operational expenditure (OPEX) (excluding externalities) of the optimal LCOE simulations per TEC was calculated using linear least-squares regression, as shown in Fig. 11. For the CAPEX the correlation coefficient was found to be 0.999978, the fit having a slope of $€2.590 \times 10^6/n_x$ and an intercept of $€4.109 \times 10^6$. For the OPEX, the correlation coefficient was 0.999637, the fit having a slope of $€1.756 \times 10^6/n_x$ and an intercept of $€6.578 \times 10^5$. The correlation coefficients indicate that the linear assumption is sound, although the non-zero intercept for the OPEX is unexpected.

Fig. 12 plots the MMAEP versus lifetime array costs for all simulations (across all optimisation studies). The curve connecting the values for the optimal simulation at each number of TECs is shown, to allow comparison to Fig. 1(a). As shown in Fig. 13, no interactions are present for the optimal 2-TEC array layout and marginal interactions are seen

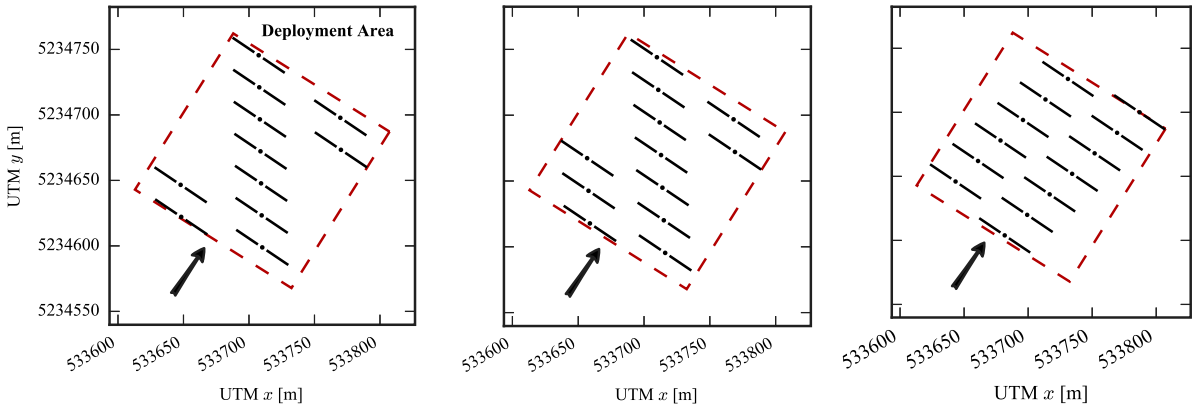

(a) 11 TECs (b) 12 TECs (c) 13 TECs

Fig. 10. Pile and rotor positions for the optimal solutions of the 11, 12 and 13 TEC optimisation studies. The deployment area is marked by the dashed line and the arrow shows the mean flow direction.

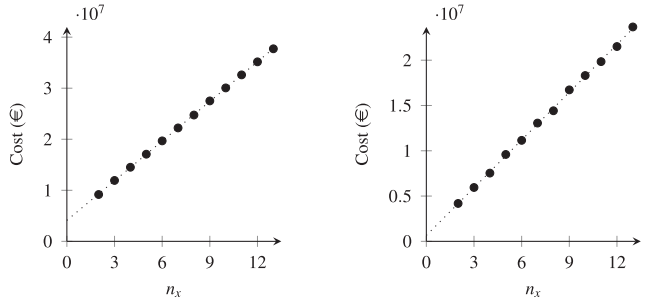

(a) CAPEX (b) OPEX

Fig. 11. Lifetime costs excluding externalities for the optimal LCOE layout of each array size (n_x). Capital costs are shown in a and operational costs in b.

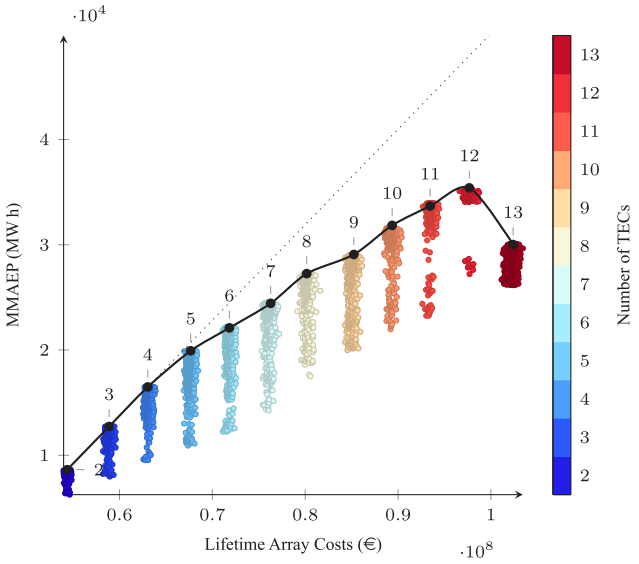

Fig. 12. MMAEP versus lifetime array costs for all simulations (across all optimisation studies). The values for the optimal layout of each array size are shown by the labelled dots on the solid line. The straight dotted line shows an approximate projection of the results if array interaction were discarded.

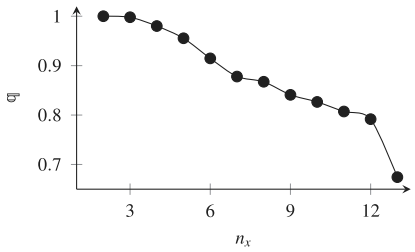

Fig. 13. Array q-factor (q) for the optimal layout of each array size (n_x).

for the optimal 3 TEC layout. Assuming the interactions of the optimal 3-TEC layout are negligible, an approximation to the theoretical non-interaction solution can be projected (shown by the dotted line in Fig. 12). Fig. 14 plots the LCOE versus MMAEP for all simulations (across all optimisation studies). The curve connecting the values for the simulations representing the optimal LCOE for each number of TECs is shown, to allow comparison to Fig. 1(b). Fig. 14 shows that significant economic benefit can be gained by allowing negative interaction between TECs. Once again assuming that the interactions for $n_x = 3$ are negligible, the optimal LCOE without interaction is €0.6621/kW h, while the optimal with interaction is €0.3453/kW h, a reduction of 47.8%.

Using the 3 TEC array as the last non-interacting value ($n_0 = 3$), the results can be compared to the hypothetical LCOE model. As additional TECs are added ($n_x > n_0$) the MMAEP increases with lifetime array cost and the LCOE reduces as the MMAEP increases. This behaviour is indicative of the $n_{0.5} \gg n_0$ solution class, illustrated by the $n_{0.5} = 15n_0$ example in Fig. 1. The behaviour changes for the optimal 13 TEC array, due to a significant increase in the interactions, as shown by Fig. 13. Subsequently, the MMAEP reduces and the LCOE increases, relative to the 12 TEC array. The change of behaviour means that the inflection point expected with the $n_{0.5} \gg n_0$ solution class was not reached and the maximum MMAEP *does* correspond to the lowest LCOE. Thus, the hypothetical model is only valid for $n_x < 13$, for this case.

To further test the efficacy of the hypothetical LCOE model, parameters of Eqs. (7) and (8) which minimise the sum of squares error to the DTOcean results, for $n_x < 13$, are sought. By definition $P_{\text{rated}} = 1.1$ MW and $C_d = 7.8096$. From the simulation results, assume $n_0 = 3$ and, using Eq. (5), $C_{\text{cap}} = 0.438$. Combining the external CAPEX cost and the intercept of Fig. 11(a) gives $c_0 = €4.511 \times 10^7$, while the slope of Fig. 11(a) gives $c_x = €2.590 \times 10^6$. From the slope of Fig. 11(b), $c_m = €8.781 \times 10^4$. To determine the remaining parameters of c_e and $n_{0.5}$, an 'Orthogonal Distance Regression' [39,40] is applied. With residual variance of 0.05915, the resulting values were $c_e = €1.403 \times 10^6$ and $n_{0.5} = 20.91$. The value for c_e is less than the input external OPEX of

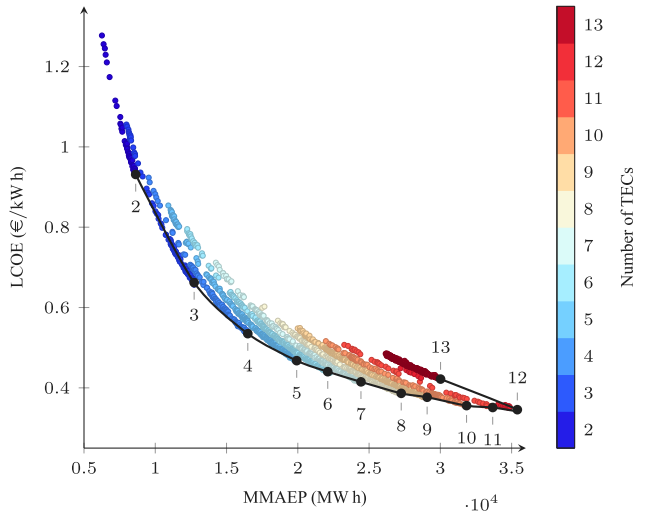

Fig. 14. LCOE versus MMAEP for all simulations (across all optimisation studies). The values for the optimal layout of each array size are shown by the labelled dots on the solid line.

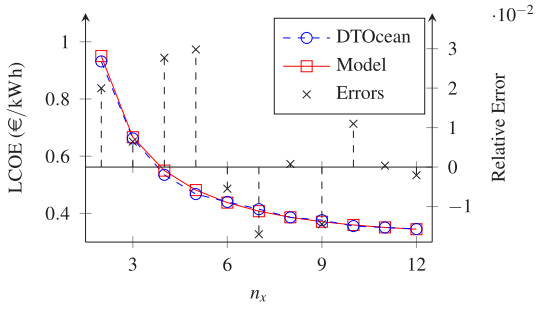

Fig. 15. Comparison of DTOcean results with calibrated LCOE model. LCOE is shown on the left hand axis, relative error on the right.

€1.81×10^6 by approximately 22.5%; some of this error may be related to the unexplained additional OPEX seen in the DTOcean results. Comparison of the calibrated model with the DTOcean results is shown in Fig. 15, including the relative error for each n_x. Overall, the model would appear to represent the DTOcean data well, for $n_x < 13$.

4. Discussion

The results of the preceding section demonstrate that the hypothetical LCOE model is valid for small tidal energy arrays, provided that the rate of change in interactions between TECs is consistent. Nonetheless, it is highly unlikely the model provides a true reflection of optimal LCOE, even when discounting the significant uncertainties inherent in the modelling process. Under such strong negative interaction, it is reasonable to assume that the TECs will be less reliable and require additional maintenance which will lead to increasing costs. A clear weakness in the LCOE model, and DTOcean, is that this relationship of cost to different levels of TEC interaction is not captured.

Developing a relationship between interactions and maintenance costs is complex. In the absence of this information, the hypothetical model can be applied to indicate the margin of investment available to achieve the same reliability as the baseline case while still returning benefits. Fig. 16 shows the hypothetical model for three levels of TEC investment, indicated by a multiplier to the capital costs per TEC, c_x. Compared to the business-as-usual value ($1\,c_x$), the capital costs per TEC can be multiplied by a factor of 3.825 to reach parity with the LCOE of the best non-interacting array (shown by the dashed horizontal line).

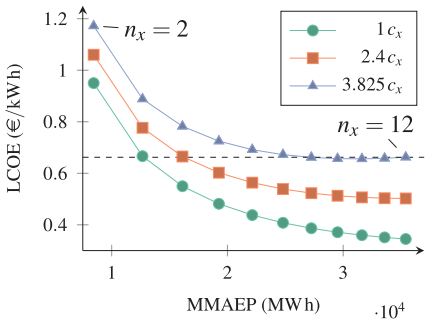

Fig. 16. Calibrated LCOE model with increasing costs per TEC (c_x) for $n_x \in [2, 12]$. The markers indicate discrete numbers of TECs and the dashed line indicates the lowest LCOE array without interactions (at $n_x = 3$).

In this case, there is no improvement in economic efficiency, but the annual energy production has increased by 178%. If the capital cost factor was 2.4, the same gain in energy production could be achieved, alongside half the economic gains over the baseline case. This amounts to a 24.1% reduction in LCOE over the most economic non-interacting array.

These results represent a radical shift in understanding of the economic impact of interactions between TECs, for small area-constrained arrays. For instance, the techno-economic model of [27] considered interactions between an array of 10 TECs, in a fixed orientation, and reported that "interactions play a decisive role in the cost of energy, which experiences increases of more than the 20%. Thus, tidal stream farms should be designed so as to attenuate the aforementioned effects, if the cost is to be minimised". In contrast, the theory developed herein indicates that by optimising TEC positions and using the available deployment area more efficiently (to include more TECs), interactions can lead to positive economic outcomes, subject to an appropriate level of investment.

The true margin of investment is strongly tied to the hypothetical model parameters, which is highly dependent on the DTOcean results. The results of this study indicate that the DTOcean hydrodynamic simulation requires further development and testing. For instance, Fig. 13 shows that the q-factor of the array increases gradually as the number of TECs increase, until the 13 TEC array when it decreases suddenly. Yet, the optimal layouts for 11, 12 and 13 TECs do not seem to differ significantly, as shown in Fig. 10. Observing this figure, the most likely cause for this sudden shift is that the hydrodynamic model does not consider the interaction of the flow with the full width of the rotors (see [22]). Thus, if the centre of a rotor is outside the wake of an upstream rotor, the proportion of the downstream rotor remaining in the wake will have no impact on its performance. The issue is exacerbated by the lack of a wake model for the turbine towers. Including the velocity at the horizontal extremes of the rotors in the power calculations and including a wake model for the turbine towers, may lead to a more consistent rate of TEC interaction, although this will inevitably increase the computational requirements of the solver. Exploring the response surface of the objective function nearby the jump in q-factor, using hypersurface visualisation [41], may help identify the dominant phenomena.

Although the channel blockage of the arrays simulated in this study remain below the scale given by [17] at which TEC arrays become "large", an assessment of the channel dynamics to ensure that a closely packed array does not significantly alter the underlying flow (which is not calculated by DTOcean) is also critical. The method of [19] offers a potential approach to examining this problem, although further development is required to ensure accurate representation of near wake interactions. Other important environmental impacts of compact array designs must also be evaluated, such as the effect on flora and fauna, sediment transport and scour.

The short row spacing in the optimal arrays revealed an interesting phenomenon, where the interactions between the TECs was less significant at higher flow velocities. This is because the flow disturbance caused by the upstream rotors is dependent on the thrust coefficient of the TEC (shown by Fig. 9), which is low at maximum flow velocity. It is important to establish whether this effect is real and exploitable or simply an artefact of the modelling assumptions. Some progress towards this goal has been made in [42], but comparisons using distances as small as modelled in this study were not considered. Clearly, the effects on reliability of such close proximity rotors also needs to be accounted for. In particular, where the rotor of one TEC is partially in the wake of another rotor, additional cyclic loads will be induced. Incorporating the impact of such effects on TEC reliability was demonstrated in [43], which used 3D CFD simulation to calculate cyclic loads on the rotor disc and equate those loads to the TEC maintenance interval.

In Fig. 14, the array with highest MMAEP corresponds to the lowest LCOE. This is a useful result for future optimisation of the array considered in this study, as it allows the position of the TECs to be fixed for highest MMAEP and the hydrodynamics need not be recalculated for the remainder of the optimisation process. This is a special case, nonetheless, and, as seen in Fig. 1(b), there are solutions where this assumption may not hold. For constrained deployment areas it is important to establish how the LCOE varies with MMAEP before deciding if optimising the TEC positioning as a separate stage is viable.

The hypothetical arrays considered as the basis for this work contain a limited set of phenomena that can affect the design of a TEC array. In particular, increasing scales of array will result in different phenomena becoming dominant. As shown in [44,45], large arrays can affect the channel dynamics such that LCOE can begin to increase as more TECs are added, without any interactions between them. Additionally, the assumption that costs increase proportionally to array size is likely to be invalid, as installation costs and OPEX have greater influence in larger arrays.

As previously stated, the DTOcean methodology cannot modify the undisturbed flows which are used in the hydrodynamic calculations. To capture these effects, the channel and regional water masses must be modelled in unison with the TECs; however, such simulations suffer high computational cost, particularly when part of an optimisation process that must accurately capture the interactions between TECs, as the DTOcean method seeks to do. An approach to address this computational burden was demonstrated by [16], which applied gradient-based optimisation and the adjoint approach to optimise many turbines with realistic flow models. This method is not appropriate for the complex balance-of-plant calculations contained in DTOcean, as the modelled technical choices (such as component selection) may not exhibit a smooth response. Where noisy cost functions (i.e. variable LCOE) are explicitly handled by the UH-CMA-ES method applied in this study, the ability of the approach in [16] to handle such cost functions is also unclear. In [19] surrogate based optimisation is used to reduce the number of simulations required to model a TEC array in a complex channel (including the effects of sediment transport). In this case, the authors noted that the method scales poorly as "the number of numerical simulations needed to build the surrogates increases proportionally with the number of design variables defined", which is not the case for the UH-CMA-ES method. More advanced surrogate modelling techniques, such as [46], may overcome these deficiencies and (assuming applicability to mixed-integer problems with noisy, non-smooth cost functions) allow optimisation of large TEC arrays, with accurate interactions, and detailed balance-of-plant modelling.

Another important factor for increasing confidence in the predictions of techno-economic models like DTOcean is quantification of uncertainty. Beyond the previously addressed modelling uncertainties, considerable uncertainty is associated with the input data. Sensitivity analysis is a proven method for quantifying uncertainty, for example [47] demonstrated application of the 'Morris' method [48] to offshore wind farm operation and maintenance cost and availability. Alternatively, uncertainty can be addressed directly within the modelling process by treating input parameters as statistical quantities [49] which are propagated through the model to provide uncertainty bounds on the outputs; establishing meaningful distributions for the inputs remains, nonetheless, somewhat challenging.

5. Conclusion

Modelling the interactions between the technical design and economic performance of an array of tidal energy converters (TECs) results in a complex multidisciplinary design optimisation (MDO) problem. A typical assumption, used to reduce the complexity of this problem, is that TECs positioned to minimise negative hydrodynamic interactions will maximise economic return. To examine the validity of this assumption for small area-constrained TEC arrays, a hypothetical analytical model for the relationship of mean mechanical annual energy production (MMAEP) to levelised cost of energy (LCOE) was developed, in Section 2.2. The model assumes that the lifetime array costs scale linearly with the number of TECs, while also capturing the effect of TEC interactions on the energy production. It was found that the model exhibits three alternative behaviours, dependent on the rate of change of energy lost to TEC interactions; only one of these behaviours showed minimum LCOE to occur at maximum MMAEP, another typical assumption in techno-economic modelling of TEC arrays.

In order to test the veracity of the LCOE model and the assumptions it depends upon, the contemporary techno-economic ocean energy array optimisation tool 'DTOcean' was modified to allow direct optimisation of TEC positions subject to minimising the LCOE of the array. As described in Section 2.4, a new optimisation architecture was developed for DTOcean alongside a new method for locating the TECs within the array deployment area. This method allows TECs to be concentrated in certain parts of the deployment area, rather than be spread across the entire domain, as was the case previously. In Section 2.5, an experiment was devised to test the hypothetical model, applying a previously verified DTOcean TEC array simulation. An optimisation was conducted for every feasible array size within a 2 ha deployment area to map the optimal LCOE and associated costs and MMAEP.

It was shown in Section 3 that the results of the DTOcean simulations emulated the hypothetical LCOE model behaviour where the LCOE reduces to a minimum, for some level of MMAEP, and then increases again. The results were consistent until the array size reached 13 TECs at which point a sharp increase in the rate of interaction between TECs occurred, resulting in MMAEP reducing and the LCOE increasing. Consequently, the expected inflection point in the model was not reached and the maximum MMAEP did lead to minimum LCOE, in this case. Within the valid range of [2, 12] TECs, the hypothetical LCOE model was calibrated to the DTOcean results for the optimal arrays, using an orthogonal distance regression to estimate two unknown parameters. It was shown that the calibrated model matched expectations well, over this range.

As discussed in Section 4, the hypothetical LCOE model is unlikely to match reality, as the impact on costs of strong negative interactions between TECs is not considered. Still, further investigation into the phenomena of compact arrays is warranted, as shown by Fig. 16, which estimates the margin of investment available to match the reliability of a non-interacting TEC while still providing benefits. For the present study, an increase in annual energy production of 178% and reduction in LCOE of 24.1% from the best non-interacting array was possible with an 140% increase in per TEC capital expenditure. Nonetheless, the true value of the available investment margin is strongly affected by uncertainties in the DTOcean tidal hydrodynamics solver. Issues include not considering the interaction of the flow with the full width of the turbine rotors, the lack of wake model for the TEC towers, the unknown accuracy of the model for close proximity interactions, and

understanding any change in the underlying channel hydrodynamics for such compact arrays.

This study indicates that small, area constrained, arrays that are subject to *negative* hydrodynamic interactions can lead to economic *benefits*, dependent on the level of investment required to ensure that TECs remain reliable. Although the uncertainties surrounding the hydrodynamic modelling transfer to the estimate of the available investment margin, these uncertainties can be easily reduced using well understood methods. The missing link is the three-way relationship between the environment, TEC reliability and costs. Without this knowledge, the true level of investment required to achieve a certain level of reliability remains unknown. TEC developers may well be willing to invest more in TEC designs (or maintenance programs) given the potential economic benefits, but the costs of understanding how much investment might be required, for a particular level of TEC interaction, would quickly nullify any gains. Thus, the onus must fall on the research community to determine the true relationship between environment, reliability and costs. If successful, the impact could be a significant increase in the economically extractable resource of small area-constrained tidal energy sites.

CRediT authorship contribution statement

Mathew B.R. Topper: Conceptualization, Methodology, Software, Validation, Formal analysis, Investigation, Resources, Data curation, Writing - original draft, Visualization. **Sterling S. Olson:** Conceptualization, Methodology, Writing - review & editing. **Jesse D. Roberts:** Writing - review & editing, Project administration, Funding acquisition.

Declaration of competing interest

The authors declare that they have no known competing financial interests or personal relationships that could have appeared to influence the work reported in this paper.

Acknowledgements

Special thanks are given to Dr. Lucy Cradden for her editorial contributions to this manuscript. Gratitude is also offered to the Centre for Ocean Energy Research at Maynooth University, Ireland, for the opportunity to present an early version of this work for their seminar series.

This work completed by Sandia National Laboratories was funded by the U.S. Department of Energy's Water Power Technologies Office. Sandia National Laboratories is a multimission laboratory managed and operated by National Technology and Engineering Solutions of Sandia, LLC., a wholly owned subsidiary of Honeywell International, Inc., for the U.S. Department of Energy's National Nuclear Security Administration under contract DE-NA0003525. This paper describes objective technical results and analysis. Any subjective views or opinions that might be expressed in the paper do not necessarily represent the views of the U.S. Department of Energy or the United States Government.

Appendix A. Optimisation under uncertainty

Following [35], the covariance matrix adaptation evolution strategy (CMA-ES) [38] is employed to solve Eq. (12). A heuristic method is preferable over a gradient based solver to avoid local minima [13] and discontinuities in the LCOE, particularly considering the discrete set of components and equipment that are available to the design modules. Nonetheless, gradient based methods can be significantly more efficient than heuristic methods for MDO optimisation problems, and further work should attempt to update the DTOcean architecture to allow them to be applied; in [35], CMA-ES was found to be the most efficient of the heuristic algorithms tested.

LCOE, as calculated by DTOcean, is subject to variability [23], which can impede the convergence of optimisers without specific treatment. In [50] an extension to the CMA-ES algorithm, known as UH-CMA-ES, added an uncertainly handling framework. It was shown that a metric for uncertainty in the function values (under some statistical measure) of an iteration of the CMA-ES algorithm could be calculated by perturbating a subset of the solutions and examining the changes of rank between the function values of the perturbated and unperturbated solutions. A positive value of the uncertainty metric indicates that uncertainty is affecting the function values.

Where uncertainty is present in the function values of an iteration, [50] suggests two mitigation strategies. These are increasing the population variance (σ) of the solution search space and increasing the number of function evaluations ($\mathbb{t}$) of the stochastic cost function, by factors of α_σ and $\alpha_\mathbb{t}$, respectively. Increasing $\mathbb{t}$ will, naturally, increase the accuracy of the statistical measure used to produce the function values, and therefore it can be increased until a desired level of accuracy is found. In DTOcean, the operations and maintenance module is responsible for all stochasticity in the LCOE and, thus, $\mathbb{t}$ is applied to the number of operational histories (see [23]) generated by the module, as shown in Fig. 4. A maximum limit on $\mathbb{t}$, $\mathbb{t}_{\max}$, may be set to avoid excessive computational time, yet this must be balanced with the desired solution accuracy. Also, given only one function evaluation may be required in the early stages of the algorithm, the median value is preferred as the statistical measure of LCOE.

In [50], UH-CMA-ES was applied to active control of instabilities in gas-turbine combustors, which is an on-line problem, meaning a final, converged, solution is not sought. To this end, α_σ and $\alpha_\mathbb{t}$ were chosen to discourage convergence. For DTOcean, a converged solution is sought. One possibility to achieve this is to set $\alpha_\sigma = 1$ (i.e. remove its influence entirely), yet this would increase the risk of premature convergence. After experiment, compromise settings were found, as follows:

$$\alpha_\sigma = \begin{cases} 1 + (\mathbb{n} + 10)^{-1} & \mathbb{t} < \mathbb{t}_{\max} \\ 1 & \text{otherwise} \end{cases}$$

$$\alpha_\mathbb{t} = 1 + 2(\mathbb{n} + 10)^{-1}$$

where $\mathbb{n}$ is the number of search space dimensions. Note, these settings were derived from the default settings of the implementation of UH-CMA-ES used in this study, 'pycma' [51]. Additional modifications were made to improve the computational efficiency of UH-CMA-ES, as detailed in Appendix B.

Appendix B. UH-CMA-ES in parallel

Within this study, a modification to the UH-CMA-ES algorithm in [50] was applied to increase its computational efficiency. In the algorithm's original form, a subset of the solutions of each CMA-ES iteration are resampled and evaluated prior to commencement of the next iteration to calculate the uncertainty metric. This approach is appropriate for serial computation, but when utilising parallel processing (under the assumption of unlimited CPU cores), an additional processing step is needed that will not fully utilise the available computational hardware. To remedy this issue, a simple moving average model is used to predict the uncertainty metric. If $\mathbb{s}_i$ is the unknown uncertainly metric for the i-th CMA-ES iteration, then

$$\mathbb{s}_i = \frac{\mathbb{s}_{i-1} + \mathbb{s}_{i-2} + \mathbb{s}_{i-3}}{3}.$$

The simulations required to calculate the uncertainly metric of the previous iteration, $\mathbb{s}_{i-1}$, are included with the simulations of the i-th CMA-ES iteration. Thus, only a single group of simulations is processed (in parallel) per iteration. The savings in computational time with the method are significant and, although the accuracy of the uncertainly metric is reduced, the effectiveness of the UH-CMA-ES algorithm was not compromised.

References

[1] Bryden IG. Tidal energy. In: Cleveland CJ, editor. Encyclopedia of energy. New York, U.S.A: Elsevier Inc.; 2004, p. 139–50. http://dx.doi.org/10.1016/B0-12-176480-X/00342-9.

[2] Teske S, editor. Achieving the Paris climate agreement goals: Global and regional 100% renewable energy scenarios with non-energy GHG pathways for +1.5 °C and +2 °C. Springer International Publishing; 2019, http://dx.doi.org/10.1007/978-3-030-05843-2.

[3] Lamy JV, Azevedo IL. Do tidal stream energy projects offer more value than offshore wind farms? A case study in the United Kingdom. Energy Policy 2018;113:28–40. http://dx.doi.org/10.1016/j.enpol.2017.10.030.

[4] Neill SP, Jordan JR, Couch SJ. Impact of tidal energy converter (TEC) arrays on the dynamics of headland sand banks. Renew Energy 2012;37(1):387–97. http://dx.doi.org/10.1016/j.renene.2011.07.003.

[5] Funke S, Kramer S, Piggott M. Design optimisation and resource assessment for tidal-stream renewable energy farms using a new continuous turbine approach. Renew Energy 2016;99:1046–61. http://dx.doi.org/10.1016/j.renene.2016.07.039.

[6] LiVecchi A, Copping A, Jenne D, Gorton A, Preus R, Gill G, et al. Powering the blue economy; exploring opportunities for marine renewable energy in maritime markets. Tech. rep. DOE/GO-1020195157, Washington, DC: US Department of Energy, Office of Energy Efficiency and Renewable Energy; 2019, p. 207. http://dx.doi.org/10.2172/1525367.

[7] Tidal and current energy resources in Ireland. Tech. rep, Sustainable Energy Ireland; 2005, URL: https://www.seai.ie/publications/Tidal_Current_Energy_Resources_in_Ireland_Report.pdf. [Accessed 15 December 2020].

[8] Neary VS, Previsic M, Jepsen RA, Lawson MJ, Yu YH, Copping AE, et al. Methodology for design and economic analysis of marine energy conversion (MEC) technologies. Tech. rep. SAND2014-9040, Sandia National Laboratories; 2014, URL: https://energy.sandia.gov/wp-content/gallery/uploads/SAND2014-9040-RMP-REPORT.pdf. [Accessed 15 December 2020].

[9] Lazard's levelized cost of energy analysis – version 11.0. Tech. rep., Lazard; 2017, p. 22, URL: https://www.lazard.com/media/450337/lazard-levelized-cost-of-energy-version-110.pdf. [Accessed 07 August 2020].

[10] De Andres A, Maillet J, Hals Todalshaug J, Möller P, Bould D, Jeffrey H. Techno-economic related metrics for a wave energy converters feasibility assessment. Sustainability 2016;8(11):1109. http://dx.doi.org/10.3390/su8111109.

[11] Martins JRRA, Lambe AB. Multidisciplinary design optimization: a survey of architectures. AIAA J 2013;51(9):2049–75. http://dx.doi.org/10.2514/1.J051895.

[12] Kroo IM. MDO for large-scale design. In: Alexandrov NM, Hussaini MY, editors. Multidisciplinary design optimization: state of the art. Society for Industrial and Applied Mathematics; 1997, p. 22–44.

[13] Perez-Moreno SS, Dykes K, Merz KO, Zaaijer MB. Multidisciplinary design analysis and optimisation of a reference offshore wind plant. J Phys Conf Ser 2018;1037:042004. http://dx.doi.org/10.1088/1742-6596/1037/4/042004.

[14] Bryden IG, Couch SJ, Owen A, Melville G. Tidal current resource assessment. Proc Inst Mech Eng A 2007;221(2):125–35. http://dx.doi.org/10.1243/09576509JPE238.

[15] Sutherland G, Foreman M, Garrett C. Tidal current energy assessment for johnstone strait, vancouver island. Proc Inst Mech Eng A 2007;221(2):147–57. http://dx.doi.org/10.1243/09576509JPE338.

[16] Funke S, Farrell P, Piggott M. Tidal turbine array optimisation using the adjoint approach. Renew Energy 2014;63:658–73. http://dx.doi.org/10.1016/j.renene.2013.09.031.

[17] Vennell R, Funke SW, Draper S, Stevens C, Divett T. Designing large arrays of tidal turbines: A synthesis and review. Renew Sustain Energy Rev 2015;41:454–72. http://dx.doi.org/10.1016/j.rser.2014.08.022.

[18] DTOcean user manual. Tech. rep., DTOcean Consortium; 2016, URL: https://dtocean.github.io/v1.0.0/index.html. [Accessed 25 May 2021].

[19] González-Gorbeña E, Pacheco A, Plomaritis TA, Ferreira Ó, Sequeira C. Estimating the optimum size of a tidal array at a multi-inlet system considering environmental and performance constraints. Appl Energy 2018;232:292–311. http://dx.doi.org/10.1016/j.apenergy.2018.09.204.

[20] du Feu R, Funke S, Kramer S, Culley D, Hill J, Halpern B, et al. The trade-off between tidal-turbine array yield and impact on flow: A multi-objective optimisation problem. Renew Energy 2017;114:1247–57. http://dx.doi.org/10.1016/j.renene.2017.07.081.

[21] Stallard T, Collings R, Feng T, Whelan J. Interactions between tidal turbine wakes: Experimental study of a group of three-bladed rotors. Phil Trans R Soc A 2013;371(1985):20120159. http://dx.doi.org/10.1098/rsta.2012.0159.

[22] Topper MBR, Olson SS, Roberts JD. Techno-economic modelling of tidal energy converter arrays in the tacoma narrows. J Mar Sci Eng 2020;8(9):646. http://dx.doi.org/10.3390/jmse8090646.

[23] Topper MB, Nava V, Collin AJ, Bould D, Ferri F, Olson SS, et al. Reducing variability in the cost of energy of ocean energy arrays. Renew Sustain Energy Rev 2019;112:263–79. http://dx.doi.org/10.1016/j.rser.2019.05.032.

[24] Sullivan P, McCombie P. Optimisation of tidal power arrays using a genetic algorithm. Proc Inst Civ Eng 2013;166(1):19–28. http://dx.doi.org/10.1680/ener.12.00011.

[25] González-Gorbeña E, Qassim RY, Rosman PC. Multi-dimensional optimisation of tidal energy converters array layouts considering geometric, economic and environmental constraints. Renew Energy 2018;116:647–58. http://dx.doi.org/10.1016/j.renene.2017.10.009.

[26] Polagye B, Previsic M, Hagerman G, Bedard R. System level design, performance, cost and economic assessment – tacoma narrows washington tidal instream power plant. Tech. rep. EPRI-TP-006 WA, Electric Power Research Institute; 2006, URL: https://www.re-vision.net/documents/System%20Level%20Design,%20Performance,%20Cost%20and%20Economic%20Assessment%20-%20Tacoma%20Narrows%20Washington%20Tidal%20In-Stream%20Power%20Plant.pdf. [Accessed 22 June 2020].

[27] Vazquez A, Iglesias G. Device interactions in reducing the cost of tidal stream energy. Energy Convers Manage 2015;97:428–38. http://dx.doi.org/10.1016/j.enconman.2015.03.044.

[28] Nielsen K. Development of recommended practices for testing and evaluating ocean energy systems. Tech. rep. T02-0.0, OES-IA Annex II Extension; 2010, URL: https://www.ocean-energy-systems.org/documents/87102_annex_ii_summery_report_august_.pdf/. [Accessed 15 December 2020].

[29] Allan G, Gilmartin M, McGregor P, Swales K. Levelised costs of wave and tidal energy in the UK: cost competitiveness and the importance of "banded" renewables obligation certificates. Energy Policy 2011;39(1):23–39. http://dx.doi.org/10.1016/j.enpol.2010.08.029.

[30] Katic I, Højstrup J, Jensen NO. A simple model for cluster efficiency. In: European wind energy association conference and exhibition. 1986. p. 407–10.

[31] Zimmerman RD, Murillo-Sanchez CE, Thomas RJ. MATPOWER: steady-state operations, planning, and analysis tools for power systems research and education. IEEE Trans Power Syst 2011;26(1):12–9. http://dx.doi.org/10.1109/TPWRS.2010.2051168.

[32] Abolghasemi MA. Simulating tidal turbines with multi-scale mesh optimisation techniques [Ph.D. thesis], London, UK: Imperial College; 2016.

[33] Stansby P, Stallard T. Fast optimisation of tidal stream turbine positions for power generation in small arrays with low blockage based on superposition of self-similar far-wake velocity deficit profiles. Renew Energy 2016;92:366–75. http://dx.doi.org/10.1016/j.renene.2016.02.019.

[34] Malki R, Masters I, Williams AJ, Croft TN. Planning tidal stream turbine array layouts using a coupled blade element momentum – computational fluid dynamics model. Renew Energy 2014;63:46–54. http://dx.doi.org/10.1016/j.renene.2013.08.039.

[35] Ruiz PM, Nava V, Topper MB, Minguela PR, Ferri F, Kofoed JP. Layout optimisation of wave energy converter arrays. Energies 2017;10(9):1262. http://dx.doi.org/10.3390/en10091262.

[36] DTOcean documentation, URL: https://dtocean.github.io/. [Accessed 15 December 2020].

[37] DTOceanPlus - history, URL: https://www.dtoceanplus.eu/About-DTOceanPlus/History. [Accessed 15 December 2020].

[38] Hansen N. The CMA evolution strategy: A tutorial. 2016, arXiv e-prints, arXiv:1604.00772.

[39] Boggs PT, Rogers JE. Orthogonal distance regression. In: Brown PJ, Fuller WA, editors. Contemporary mathematics, vol. 112. Providence, Rhode Island, U.S.A: American Mathematical Society; 1990, p. 183–94. http://dx.doi.org/10.1090/conm/112.

[40] Virtanen P, Gommers R, Oliphant TE, Haberland M, Reddy T, Cournapeau D, et al. SciPy 1.0: fundamental algorithms for scientific computing in python. Nat Methods 2020;17:261–72. http://dx.doi.org/10.1038/s41592-019-0686-2.

[41] Simionescu P, Beale D. Visualization of hypersurfaces and multivariable (objective) functions by partial global optimization. Vis Comput 2004;20(10):665–81. http://dx.doi.org/10.1007/s00371-004-0260-4.

[42] Olson SS, Topper MB, Chartrand CC, James SC, McWilliams S, Jones CA, et al. The limits of reduced order current energy converter modeling. In: Offshore Technology Conference. Houston, Texas, USA: 2020. http://dx.doi.org/10.4043/30704-MS.

[43] Adams N, Ranford D, Livingston D. Modelling and optimisation of tidal arrays. In: EWTEC. Southampton, UK: 2011. p. 8.

[44] Culley D, Funke S, Kramer S, Piggott M. Integration of cost modelling within the micro-siting design optimisation of tidal turbine arrays. Renew Energy 2016;85:215–27. http://dx.doi.org/10.1016/j.renene.2015.06.013.

[45] Goss ZL, Coles DS, Piggott MD. Identifying economically viable tidal sites within the alderney race through optimization of levelized cost of energy. Phil Trans R Soc A 2020;378(2178):20190500. http://dx.doi.org/10.1098/rsta.2019.0500.

[46] Neshat M, Abbasnejad E, Shi Q, Alexander B, Wagner M. Adaptive neuro-surrogate-based optimisation method for wave energy converters placement optimisation. In: Gedeon T, Wong KW, Lee M, editors. Neural information processing. Lecture notes in computer science, vol. 11954, Cham: Springer; 2019, p. 353–66. http://dx.doi.org/10.1007/978-3-030-36711-4_30.

[47] Martin R, Lazakis I, Barbouchi S, Johanning L. Sensitivity analysis of offshore wind farm operation and maintenance cost and availability. Renew Energy 2016;85:1226–36. http://dx.doi.org/10.1016/j.renene.2015.07.078.

[48] Morris MD. Factorial sampling plans for preliminary computational experiments. Technometrics 1991;33(2):161–74. http://dx.doi.org/10.1080/00401706.1991.10484804.

[49] Roy CJ, Oberkampf WL. A comprehensive framework for verification, validation, and uncertainty quantification in scientific computing. Comput Methods Appl Mech Engrg 2011;200(25):2131–44. http://dx.doi.org/10.1016/j.cma.2011.03.016.

[50] Hansen N, Niederberger A, Guzzella L, Koumoutsakos P. A method for handling uncertainty in evolutionary optimization with an application to feedback control of combustion. IEEE Trans Evol Comput 2009;13(1):180–97. http://dx.doi.org/10.1109/TEVC.2008.924423.

[51] Hansen N, Akimoto Y, Baudis P. pycma. 2019, http://dx.doi.org/10.5281/zenodo.2651072.